



**HAL**  
open science

# Lorentz-invariant topological structures of the electromagnetic field in a Fabry-Perot resonant slit grating

Marina Yakovleva, Jean-Luc Pelouard, Fabrice Pardo

► **To cite this version:**

Marina Yakovleva, Jean-Luc Pelouard, Fabrice Pardo. Lorentz-invariant topological structures of the electromagnetic field in a Fabry-Perot resonant slit grating. *Physical Review A*, 2022, 106 (6), pp.L060201. 10.1103/PhysRevA.106.L060201. hal-03889141

**HAL Id: hal-03889141**

**<https://cnrs.hal.science/hal-03889141>**

Submitted on 7 Dec 2022

**HAL** is a multi-disciplinary open access archive for the deposit and dissemination of scientific research documents, whether they are published or not. The documents may come from teaching and research institutions in France or abroad, or from public or private research centers.

L'archive ouverte pluridisciplinaire **HAL**, est destinée au dépôt et à la diffusion de documents scientifiques de niveau recherche, publiés ou non, émanant des établissements d'enseignement et de recherche français ou étrangers, des laboratoires publics ou privés.



Distributed under a Creative Commons Attribution - NonCommercial - ShareAlike 4.0 International License

## Lorentz-invariant topological structures of the electromagnetic field in a Fabry-Perot resonant slit grating

Marina Yakovleva <sup>\*</sup>, Jean-Luc Pelouard , and Fabrice Pardo <sup>†</sup>

Université Paris-Saclay, CNRS, Centre de Nanosciences et de Nanotechnologies, 91120, Palaiseau, France



(Received 25 August 2022; accepted 15 November 2022; published 7 December 2022)

It is commonly assumed that the most correct description of the electromagnetic world is the abstract one, and that topological constructs, such as lines of force are not covariant. In this Letter, we show that for a  $y$ -invariant system with a  $p$ -polarized electromagnetic field, it is possible to construct absolute (i.e., Lorentz invariant) lines in  $(t, x, z)$  space-time, which we call *electric spaghettis* (ESs). The electromagnetic field is fully described by the ES topology that transcends the limit between space and time, plus a new invariant, the characteristic parameter  $\eta$ . In a Fabry-Perot resonant slit grating, three ES patterns can be distinguished, corresponding to three regions: null straight lines in plane-wave regions, rounded rhombi in the interference region inside the grating, and Bernoulli's logarithmic spiral patterns—the first ever described fractals—in the funneling region.

DOI: [10.1103/PhysRevA.106.L060201](https://doi.org/10.1103/PhysRevA.106.L060201)

Faraday's concept of lines of force [1,2] was the first topology describing the electromagnetic field. However, with our modern point of view, this topological construct is not Lorentz invariant, and it is commonly assumed that *the most correct description of the electromagnetic field is the abstract one* [3,4]. Nevertheless, few attempts to define a space-time topology of the electromagnetic field have been performed. The idea of tubes of flux, a space-time generalization of Maxwell's concept [2], was described, for example, by Misner *et al.* in their book *Gravitation* [5]. Unfortunately, it only leads to a schematic and does not construct well-defined space-time topological structures. A frequent approach of field two-forms is to separate space and time [6,7], losing the Lorentz invariance. Absolute representations of two-forms were given only for simple cases, by Jancewicz for an electric charge [8] and by Warnick and Russer for the case of a propagating plane wave [9].

In an attempt to construct a Lorentz-invariant topology of the electromagnetic field, Gratus [10] has suggested to consider fixed-coordinate space slices of the four-dimensional (4D) space-time. A space slice, being arbitrary in the general case, is canonical for a  $y$ -invariant  $p$ -polarized electromagnetic field. In this case, the Maxwell's two-form becomes a simple two-form, and its pullback onto any arbitrary  $y = \text{Const}$  plane defines lines in the two- plus one-dimensional (2+1D) space-time. There is similarity between these lines and Faraday's lines of force for a static field in three-dimensional (3D) space. The topology by itself defines at any point (or event) two directional parameters, and a third parameter is necessary to completely describe the field, either the value of the electrostatic potential or the field amplitude (that can be illustrated by the density of lines). However, this field description by a topology plus a parameter cannot be

straightforwardly generalized from 3D space to 2 + 1D space-time, mainly because of the peculiarity of null-like directions in the latter. In the absence of charge, it is evident that field lines never end in 3D space, but this is not an established fact in 2 + 1D space-time.

In this Letter, we show that a  $y$ -invariant  $p$ -polarized electromagnetic field (i.e., satisfying the Maxwell's and constitutive equations) can be fully described by an absolute topology of lines in  $(t, x, z)$  space-time [named here the *electric spaghettis* (ESs)] with a new Lorentz-invariant scalar measure on them, the  $\eta$  parameter. This topology is studied in detail for an infinite line of charge and for a Fabry-Perot resonant slit grating. The latter exhibits three specific topological ES structures: the single plane-wave region high above the grating, the two interfering plane-wave regions inside the grating, and the funnel region in the near field of the grating. In the funneling region a fractal topological structure around null field events is observed. These endless ES whirls, which seem to contradict the absence of magnetic charge [10], are justified here by a careful analysis.

For a  $y$ -invariant  $p$ -polarized field, the six components of Faraday's  $F = (-\mathbf{E}, \mathbf{B})$  or Maxwell's  $\mathcal{G} = (\mathbf{H}, \mathbf{D})$  2-forms [5,11] reduce to three components with

$$\mathcal{G} = H_y dt \wedge dy + D_x dy \wedge dz + D_z dx \wedge dy, \quad (1)$$

in natural units ( $c = 1$ ). Factoring out  $dy$ , this 2-form can be written as  $\mathcal{G} = \phi_e \wedge dy$  with  $\phi_e$  the 1-form

$$\phi_e = H_y dt + D_z dx - D_x dz. \quad (2)$$

The dual of this 1-form is the vector,

$$\boldsymbol{\tau}_S = H_y \partial_t - D_z \partial_x + D_x \partial_z. \quad (3)$$

This vector defines integral curves, the ESs, that are absolute topological structures in 2 + 1D space-time: a given line connects the same set of events, independently of any frame of reference. A tensorial approach and the explicit Lorentz transform calculation is given in the Supplemental Material

<sup>\*</sup>marina.yakovleva@c2n.upsaclay.fr

<sup>†</sup>fabrice.pardo@c2n.upsaclay.fr

[12]. Starting from any event  $s_0$ , the line  $ES(s_0)$  can be built using the parametric equation,

$$s(\eta) = s_0 + \int_0^\eta \tau_S d\eta. \quad (4)$$

The 2-form Eq. (1) that allows to compute the electric flux  $\mathcal{G}(\sigma)$  on any oriented surface element  $\sigma$  in 3 + 1D space-time (with a density  $D_x$  on  $\partial_y \wedge \partial_z$  surface,  $D_z$  on  $\partial_x \wedge \partial_y$  surface, and  $H_y$  on  $\partial_t \wedge \partial_y$  surface), reduces to the 1-form  $\phi_e$ , which, being applied to any vector  $\mathbf{a}$  in 2 + 1D space-time, gives the electric flux value  $\varphi_e(\mathbf{a}) = \mathcal{G}(\mathbf{a} \wedge \partial_y)$  on this vector. The electric flux on a spaghetti segment  $ES_{e_1 e_2}$  from the event  $e_1 = s(\eta_1)$  to the event  $e_2 = s(\eta_2)$  has then the value,

$$\varphi_e(ES_{e_1 e_2}) = \int_{\eta_1}^{\eta_2} (H^2 - D^2) d\eta. \quad (5)$$

In this equation, the electric flux value  $\varphi_e$  and the  $H^2 - D^2$  factor are both Lorentz invariant. Hence,  $\eta(ES_{e_1 e_2}) = \eta_2 - \eta_1$  is actually a new Lorentz invariant.

From a topological point of view, a set of ESs can be constructed to cover any region of the 2 + 1D space-time with a nonzero electromagnetic field. Furthermore, an oriented segment of ES can be labeled with three quantities: (1) its interval length (but only if the segment is purely timelike or spacelike), (2) its electric flux  $\varphi_e$ , and (3) its characteristic parameter  $\eta$ .

Unlike world lines of physical objects, which are always timelike, ESs transcend the boundary between time and space directions. Some parts of the same ES can be timelike, spacelike, and even lightlike. The particular case where ESs are contained in a light cone requires some attention as  $H^2 - D^2$ , the interval and the electric flux are all equal to zero. In contrast, the  $\eta$  value of a nondegenerate (i.e., not reduced to a point) ES segment is never zero, and has a sign fixed by the orientation of ES. If an arbitrary inertial frame of reference is chosen, the components of the electromagnetic field can be obtained from the ES topology and the  $\eta$  value using Eq. (4),

$$H_y = \frac{ds_t}{d\eta}, \quad D_z = -\frac{ds_x}{d\eta}, \quad D_x = \frac{ds_z}{d\eta}, \quad (6)$$

where  $s_t, s_x, s_z$  are the ES coordinates. The smaller the field, the larger the  $\eta$  value. It may seem rather counterintuitive, but the ES characteristic parameter  $\eta$  is an absolute extensive physical property of ESs.

Figure 1(a) shows the case of a linear constant density of charge  $\lambda$  along the  $y$  direction. The world line of each charge is a straight line along the  $Ot$  axis, and this axis represents all charges in 2 + 1D space-time ( $t, x, z$ ). ESs appear as concentric green circles centered around the  $Ot$  line. Every ES circle contains the same electric flux value  $\varphi_e = \lambda$ . The pink radial surfaces are zero-electric flux surfaces (ZEFSS). They are perpendicular to the ESs and start on the  $Ot$  charge world line. The electric flux on them is zero.

At first glance, Fig. 1(a) is a picture of equipotential lines (green circles, which are indeed cylinders along the  $y$  axis in 4D space-time) and electric-field strength lines, extended in the time direction (pink surfaces). However, the concept of equipotential lines is frame dependent: in a different frame of reference, a magnetic field would appear, and both the electric field and the equipotential lines would change. In contrast, ESs and ZEFSSs are absolute, connecting the same

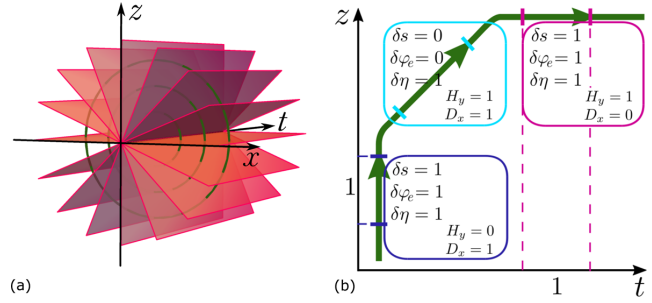


FIG. 1. (a) A  $t$ -invariant (electrostatic) case: an  $Oy$  charged line with the  $Ot$  world line. Green circles: ESs and pink surfaces: ZEFSSs. (b) A non- $t$ -invariant case: ES (green line) with purely an electric-field part ( $z$  direction, dark-blue frame), plane-wave part (null-like direction, light-blue frame), and purely magnetic field ( $t$  direction, purple frame). The ES topology is absolute, the interval values  $\delta s$ , the flux values  $\delta\varphi_e$ , and the characteristic parameter values  $\delta\eta$  are all absolute, independent of the reference frame. In contrast,  $H_y$  and  $D_x$  depend on the axis choice ( $t, z$ ) with Eqs. (3) and (6). When ES is null-like, only the parameter  $\eta$  has a nonzero value, able to describe the electromagnetic field in this region.

set of events, independently of any frame of reference. The  $\eta$  value calculated between two events of a given ES is absolute, independent of the choice of a reference frame. The field components, which are relative, can be simply derived from the ES topology and the parameter  $\eta$ , using Eq. (6). In this electrostatic example,  $\varphi_e$  has the same value  $\lambda$  on all circles. By contrast,  $\eta = 4\pi^2 R^2 / \lambda$  is proportional to the square of the radius  $R$ . The usefulness of the parameter  $\eta$ , not obvious in this example, is crucial when the ES part belongs to a light cone as shown in Fig. 1(b) where an ES is successively spacelike, null-like, and timelike, transcending the distinction between space and time.

The Fabry-Perot resonant slit grating system studied in this Letter consists of a perfectly conducting metal with slits parallel to the  $y$  direction [Fig. 2(a)], excited at normal incidence by a  $p$ -polarized plane wave (i.e., with the magnetic field oriented along the  $y$  direction). The grating period is  $L = \pi$ , that is, half the wavelength  $\Lambda = 2\pi$  ( $c = 1$ ), so all the diffracted waves are evanescent. The slit width is arbitrarily chosen as  $w = L/6$ . This system is known for perfect transmission of incident radiation [13] with a funneling mechanism [Fig. 2(b)] that can be understood by the magnetoelectric interference between the incident and the evanescent fields [14]. The Fabry-Perot resonance condition corresponding to total transmission and no reflection is obtained for a slit height  $h$  equal to  $h = h_0 + n \Lambda/2$  with  $h_0 \approx 0.417\Lambda$ , and  $n$  is an arbitrary integer. The value of  $h_0$  is slightly smaller than  $\Lambda/2$  as the phase of the internal reflection is not exactly  $\pi$ . The value of  $h = 0.917\Lambda$  was chosen for a clear view of the interference pattern inside the slits.

Several numerical techniques based on Eqs. (4) and (5) were used to compute ESs and ZEFSSs. Full descriptions of these and code books are presented in the Supplemental Material [12]. Figure 2(d) shows ESs crossing the line  $z = -h/2, x = -2w/5$ . The median plane of a slit is a special place because the  $D_z$  component is here equal to zero, and the ESs remain localized on this plane [see Eq. (3) and Fig. 2(c)].

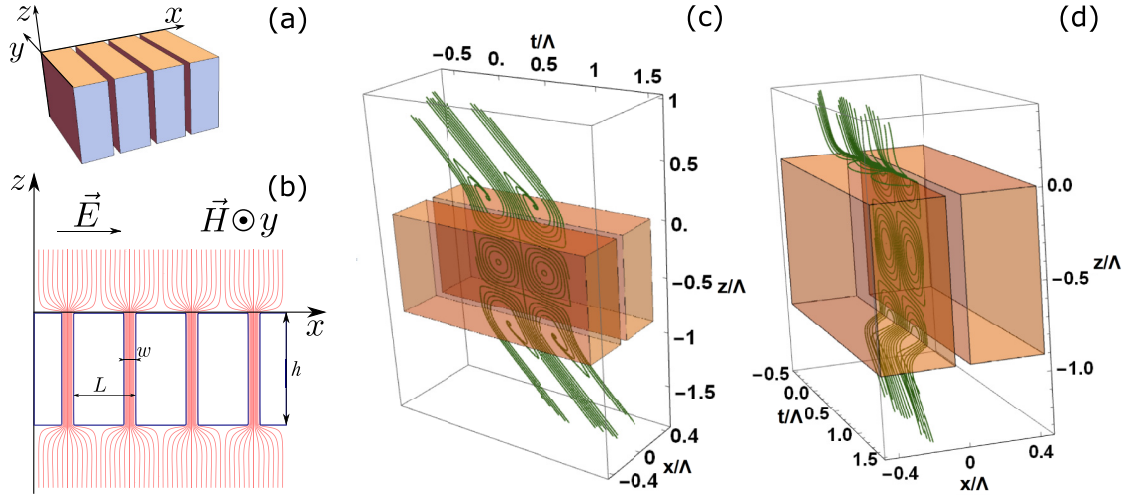


FIG. 2. (a) Slit grating, invariable in the  $y$  direction, made in a perfect conductor. (b) Time-averaged Poynting vector lines in the resonant case,  $p$ -polarized normally incident monochromatic wave. (c) ESs in the central plane of a slit. (d) ESs crossing the line  $z = -h/2$ ,  $x = -2w/5$ .

These ESs are also plotted in Fig. 3 along with ZEFs lines. As there are no electric charges in the considered region, the electric flux is constant between two neighboring bold ZEFs lines, and the density of these lines in the  $t$  direction corresponds to the value of the field component  $H_y$ , and the density in the  $z$  direction corresponds to the value of the field component  $D_x$ .

Far from the slits where a single plane wave propagates  $D_x = H_y$ , the ESs are straight null-like lines according to Eq. (3). Inside a slit where two plane waves interfere, concentric patterns of rounded rhombi are observed. The field is purely electric when the ESs (green lines) are parallel to the  $z$  direction and purely magnetic when they are parallel to the  $t$  direction. Owing to the resonance inside the slit, the electric flux density in this region is six times higher than on

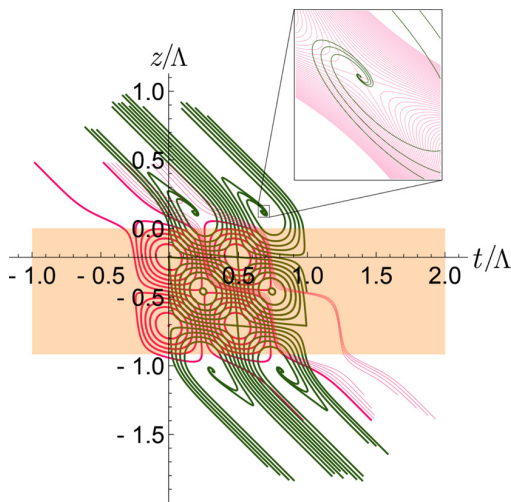


FIG. 3. Plot of the ES (green) and ZEFs (red) lines on the median plane for one time period. The orange zone corresponds to the slit area. The electric flux is constant between two thick red ZEFs lines and between two thin red lines with a factor of  $1/6$ . The inset: zoom of the whirl zone with very small flux steps between ZEFs lines.

the plane-wave region. This is clearly depicted in Fig. 3: in the slit region, there are six ZEFs lines over a half-period in time, whereas in the upper part of the figure (plane-wave region), there is only one bold ZEFs line. Compared with the interference of two identical plane waves [15], the rounded squares are slightly distorted. This is because the amplitude of the wave from bottom to top is smaller than that from top to bottom.

In the funneling region, ESs form whirls that are centered on zero field events. They seem to contradict the principle that tubes of flux with no charge never end [5], so they require detailed analysis. The field in the funneling region is the superposition of the incoming plane wave and of a series of diffracted evanescent waves. For simplicity, let us restrict the continuation of the study to only the first diffracted wave. In this model, the incident plane wave has amplitude  $\cos(z+t)$ , and the evanescent wave has amplitude  $a \exp(-\sqrt{3}z) \sin(t) \cos(2x)$  where the amplitude  $a = 1.091$  and the phase  $\pi/2$  are obtained numerically (see the Supplemental Material [12]). The ES-ZEFs pattern of this interference is plotted as, respectively, green and red lines in Fig. 4(a). The pattern of this simplified model is similar to the

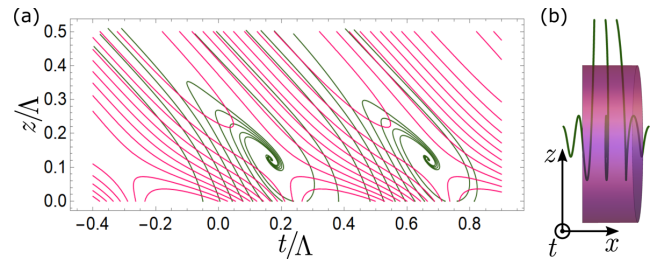


FIG. 4. (a) ESs (green) and ZEFs lines (red) in the case of interference of the plane wave and two evanescent ones (with equal amplitudes and opposite propagation directions along the  $x$  axis). (b) Space-time camembert box (also known as a pill box) with incoming, never outgoing ESs at  $x = 0$ . Other ESs are outgoing through one of the sides.

one observed in Fig. 3. The whirls are centered on zero-field points  $H_y = D_x = 0$ .

Using a linear approximation of the field components around the zero-field points ( $t_0 = \pi/3 + p/2$ ,  $z_0 = 0.7736$ ), the parametric equation of an ES is (see the Supplemental Material [12]),

$$\begin{pmatrix} t(\eta) - t_0 \\ z(\eta) - z_0 \end{pmatrix} = z_0 \begin{pmatrix} 0 & \beta \\ 1 & -\alpha \end{pmatrix} \begin{pmatrix} \cos \lambda_i \eta \\ \sin \lambda_i \eta \end{pmatrix} e^{-\lambda_r \eta}, \quad (7)$$

$$x(\eta) = x_0 e^{2\lambda_r \eta}, \quad (8)$$

where  $\lambda_i = \sqrt{(3 \sin z_0 + \frac{\cos z_0}{\sqrt{3}})(\sin z_0 - \frac{\cos z_0}{\sqrt{3}})}$ , and  $\lambda_r = \sin z_0 - \frac{\cos z_0}{\sqrt{3}}$ . For  $x_0 = 0$  this is an affine transformation of a curve, named *spira mirabilis* by Bernoulli three centuries ago [16]. It is an endless spiral, the first fractal curve ever studied. And this is the key of the paradox that ESs should never end. They never end indeed. Each loop of the ES toward the center corresponds to  $2\pi/\lambda_i$  change in the parameter  $\eta$  whereas the radius decreases by a factor of  $\exp(-2\pi\lambda_r/\lambda_i) = 0.12$ .

The ES bundles in a vacuum makes tubes of magnetic flux, corresponding to the Faraday 2-form  $E_x dx \wedge dt + E_z dz \wedge dt + B_y dz \wedge dx$  (see the Supplemental Material [12]). As there are no magnetic charges, any tube entering on a given closed surface  $\Sigma$  of space-time  $(t, x, z)$  must exit somewhere on the same surface. The observed endless ESs do not contradict this law because they are restricted to  $x = 0$  plane, having zero measure on the surface  $\Sigma$ . Considering the camembert box (also known as the pill box) in Fig. 4(b), the incoming ESs at the periphery exit through the sides of the disk, thus, defining tubes of constant magnetic flux.

To conclude, we demonstrated that a  $y$ -invariant  $p$ -polarized electromagnetic field, which is usually represented by three field components (as  $H_y, D_z, D_x$ , relative to a frame of reference), can be represented in an absolute way. In a flat space-time, the qualifier *absolute* is synonymous with the *Lorentz invariant*. It should be noted that the content of this

Letter can be extended to a curved space-time, provided that there is translation symmetry along the  $y$  direction. The electromagnetic field can be represented by unique and absolute structures, the Ss, measured by the absolute parameter  $\eta$ . The surfaces perpendicular to ESs (the ZEFSSs) are also absolute space-time structures. Contrary to the world lines of physical objects, which are always timelike, ESs and ZEFSSs transcend the limit between space and time. Any segment of ES is characterized by two absolute electromagnetic quantities: its electric flux  $\varphi_e$ , and its characteristic parameter  $\eta$ . Despite its counterintuitive nature (the larger it is, the smaller the field is),  $\eta$  is a parameter that makes sense because it can describe the electromagnetic field everywhere. In contrast, the flux and interval values, which are zero on null-like segments of ESs, cannot describe the electromagnetic field everywhere. ESs with  $\eta$  milestones written on them form a complete representation of the electromagnetic world in the  $2 + 1D$   $y$ -invariant space-time, giving in any inertial frame of reference  $(t, x, z)$ , the field components  $H_y, D_z, D_x$ .

We explored the ES topology of a Fabry-Perot resonant slit grating. In the plane-wave region ESs are straight light lines with an electric field equal to the magnetic field. Inside the slits, the ESs are mainly rounded rhombi, corresponding to the interference of two plane waves with purely  $H_y$  zones and purely  $D_x$  zones. The funneling region is of particular interest with ESs having the fractal behavior of logarithmic spirals. They correspond to the interference of the incident wave with the evanescent waves diffracted by the slit grating.

ESs illustrate the profound unity of electric and magnetic fields and give them a topological structure that can be studied for itself, opening a new field of research. Also, instead of considering field components, which are related to an arbitrary frame of reference, the description of the field as an absolute topology in space-time with absolute measure  $\eta$  is a radical change in the conceptual approach to the electromagnetic world. This not only has philosophical and educational consequences, but also suggests new computational approaches.

- 
- [1] M. Faraday, *London, Edinburgh, and Dublin Philos. Mag. J. Sci.* **3**, 401 (1852).
- [2] J. C. Maxwell, *London, Edinburgh, and Dublin Philos. Mag. J. Sci.* **21**, 161 (1861).
- [3] R. P. Feynman, R. B. Leighton, and M. Sands, *The Feynman Lectures on Physics: Mainly Electromagnetism and Matter* (Addison-Wesley, Reading, reprinted, 1977), Vol. 2.
- [4] F. Dyson, in *The Second European Conference on Antennas and Propagation, EuCAP 2007* (EICC, Edinburgh, UK, 2007), pp. 1–6, doi: [10.1049/ic.2007.1146](https://doi.org/10.1049/ic.2007.1146).
- [5] C. W. Misner, K. S. Thorne, and J. A. Wheeler, *Gravitation* (W. H. Freeman, Princeton University Press, 1973).
- [6] G. A. Deschamps, *Proc. IEEE* **69**, 676 (1981).
- [7] K. F. Warnick and P. H. Russer, *Prog. In Electromag. Res.* **148**, 83 (2014).
- [8] B. Jancewicz, *Multivectors and Clifford Algebra in Eectrodynamics* (World Scientific, Singapore, 1989).
- [9] K. F. Warnick and P. Russer, *Turkish J. Electrical Eng. Comput. Sci.* **14**, 153 (2006).
- [10] J. Gratus, [arXiv:1709.08492](https://arxiv.org/abs/1709.08492).
- [11] A. Stern, Y. Tong, M. Desbrun, and J. E. Marsden, Geometric computational electrodynamics with variational integrators and discrete differential forms, in *Geometry, Mechanics, and Dynamics*, Fields Institute Communications, Vol. 73, edited by D. Chang, D. Holm, G. Patrick, and T. Ratiu (Springer, New York, NY, 2015), pp. 437–475, doi: [10.1007/978-1-4939-2441-7\\_19](https://doi.org/10.1007/978-1-4939-2441-7_19).
- [12] See Supplemental Material at <http://link.aps.org/supplemental/10.1103/PhysRevA.106.L060201> for detailed calculations and proofs.
- [13] P. N. Stavrinou and L. Solymár, *Opt. Commun.* **206**, 217 (2002).
- [14] F. Pardo, P. Bouchon, R. Haïdar, and J.-L. Pelouard, *Phys. Rev. Lett.* **107**, 093902 (2011).
- [15] F. Pardo, in *Séminaire Général du Département de Physique* (École Polytechnique, Palaiseau, France, 2016), <https://youtu.be/PAne0N6PtI8>.
- [16] Ø. Hammer, *The Perfect Shape* (Springer, Berlin, 2016), pp. 33–38.

# Supplemental material to the letter Lorentz-invariant topological structures of the electromagnetic field, the Fabry-Perot resonant slit-grating case.

Marina Yakovleva,<sup>1,\*</sup> Jean-Luc Pelouard,<sup>1</sup> and Fabrice Pardo<sup>1,†</sup>

<sup>1</sup> *Université Paris-Saclay, CNRS, Centre de Nanosciences et de Nanotechnologies, 91120, Palaiseau, France.*

(Dated: November 15, 2022)

## I. CALCULATION OF WHIRL

The flux and field components of the interference of a plane wave and the first stationary evanescent wave diffracted by a grating with period  $L = \Lambda/2$ , wavelength  $\Lambda = 2\pi$ , are

$$\varphi_e = \sin(z+t) - a \exp(-\sqrt{3}z) \cos t \cos 2x \quad (1)$$

$$H_y = \cos(z+t) + a \exp(-\sqrt{3}z) \sin t \cos 2x \quad (2)$$

$$D_x = -\cos(z+t) - a\sqrt{3} \exp(-\sqrt{3}z) \cos t \cos 2x \quad (3)$$

$$D_z = 2a \exp(-\sqrt{3}z) \cos t \sin 2x \quad (4)$$

with  $a = 1.091$  for the resonant slit grating we consider.

The ES-ZEFS pattern of this interference at  $x = 0$  (corresponds to the middle plane of a slit for the grating described above) is plotted as green and red lines in Fig. 1. The pattern of this simplified model is very similar to the one observed in Fig. 4 of the main text.

The whirls in Fig. 1 are centered on zero-field points  $H_y = E_x = 0$ , corresponding to equations:

$$\tan t_0 = \sqrt{3} \quad (5)$$

$$\frac{\cos z_0}{\sqrt{3}} - \sin z_0 + a \exp(-\sqrt{3}z_0) = 0 \quad (6)$$

with solution ( $t_0 = \pi/3, z_0 = 0.7736$ ).

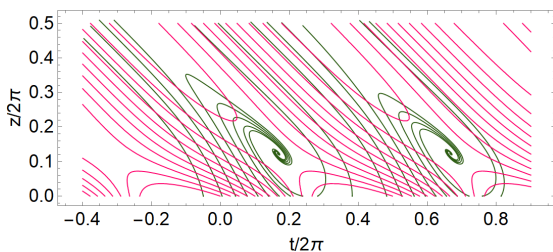


FIG. 1. ESs (green) and ZEFS-lines (red) in the case of interference of the plane wave and two evanescent ones (with equal amplitudes and opposite propagation directions along  $x$  axis.).

The asymptotic character of the whirls can be obtained by a linear approximation ( $t = t_0 + t', x = x', z = z_0 + z'$ ) of the field around the point  $(t_0, 0, z_0)$ :

$$\begin{pmatrix} H_y \\ D_x \end{pmatrix} = \lambda_i A \begin{pmatrix} t' \\ z' \end{pmatrix} \quad (7)$$

$$D_z = \lambda_x x' \quad (8)$$

with

$$A = \begin{pmatrix} -2\alpha + \beta & -\beta \\ \beta & \beta \end{pmatrix} \quad (9)$$

$$\lambda_i = \sqrt{(3 \sin z_0 + \frac{\cos z_0}{\sqrt{3}})(\sin z_0 - \frac{\cos z_0}{\sqrt{3}})} \quad (10)$$

$$\lambda_i \alpha = \sin z_0 + \frac{\cos z_0}{\sqrt{3}} \quad (11)$$

$$\lambda_i \beta = 2 \sin z_0 \quad (12)$$

$$\lambda_x = \lambda_i (-2\alpha + 2\beta). \quad (13)$$

The factor  $\lambda_i$  will appear later as the angular frequency for ES  $\eta$  parameter. From these equations we obtain

$$\beta^2 = 1 + \alpha^2. \quad (14)$$

Applying Eq.(6) from the main part, ES equations becomes:

$$\frac{d}{d\eta} \begin{pmatrix} t' \\ z' \end{pmatrix} = \lambda_i A \begin{pmatrix} t' \\ z' \end{pmatrix} \quad (15)$$

$$\frac{dx'}{d\eta} = -\lambda_x x'. \quad (16)$$

The solution of this system of differential equations is

$$\begin{pmatrix} t'(\eta) \\ z'(\eta) \end{pmatrix} = e^{\lambda_i \eta A} \begin{pmatrix} t'(0) \\ z'(0) \end{pmatrix} \quad (17)$$

$$x'(\eta) = e^{-\lambda_x \eta} x'(0) \quad (18)$$

where the exponential of matrix  $\lambda_i \eta A$  can be obtained from its eigenvalues  $\lambda_{\pm}$  and eigenvectors matrix  $V$ :

$$\exp(\lambda_i \eta A) = V \begin{pmatrix} \exp(\lambda_+ \eta) & 0 \\ 0 & \exp(\lambda_- \eta) \end{pmatrix} V^{-1} \quad (19)$$

where

$$\lambda_i A V = V \begin{pmatrix} \lambda_+ & 0 \\ 0 & \lambda_- \end{pmatrix}. \quad (20)$$

\* marina.yakovleva@c2n.upsaclay.fr

† fabrice.pardo@c2n.upsaclay.fr

Explicitly

$$\lambda_{\pm} = \lambda_r \pm i\lambda_i \quad (21)$$

with

$$\lambda_r = (\beta - \alpha)\lambda_i = \lambda_x/2 \quad (22)$$

and

$$V = \begin{pmatrix} -\alpha + i & -\alpha - i \\ \beta & \beta \end{pmatrix} \quad (23)$$

$$V^{-1} = \frac{1}{2\beta} \begin{pmatrix} -i\beta & 1 - i\alpha \\ i\beta & 1 + i\alpha \end{pmatrix}. \quad (24)$$

Equation (19) can be rewritten as

$$\exp(\lambda_i \eta A) = e^{\lambda_r \eta} \left( \cos(\lambda_i \eta) + \sin(\lambda_i \eta) V \begin{pmatrix} i & 0 \\ 0 & -i \end{pmatrix} V^{-1} \right).$$

Calculating

$$V \begin{pmatrix} i & 0 \\ 0 & -i \end{pmatrix} V^{-1}$$

and considering the starting point  $t'(0) = 0, x'(0) = x_s, z'(0) = z_s$ , we obtain

$$\begin{pmatrix} t'(\eta) \\ z'(\eta) \end{pmatrix} = z_s e^{\lambda_r \eta} \begin{pmatrix} 0 & -\beta \\ 1 & \alpha \end{pmatrix} \begin{pmatrix} \cos \lambda_i \eta \\ \sin \lambda_i \eta \end{pmatrix} \quad (25)$$

$$x'(\eta) = x_s e^{-2\lambda_r \eta} \quad (26)$$

The equation (25) is an affine transformation of the logarithmic spiral:

$$\begin{pmatrix} t''(\eta) \\ z''(\eta) \end{pmatrix} = e^{\lambda_r \eta} \begin{pmatrix} \cos \lambda_i \eta \\ \sin \lambda_i \eta \end{pmatrix} \quad (27)$$

This curve, named *spira mirabilis* by Bernoulli three centuries ago, is a spiral that never ends, the first fractal curve ever studied. For each loop toward the center, corresponding to a decrease in parameter  $\eta$  equal to  $-2\pi/\lambda_i$ , the radius is decreased by a factor of  $\exp(-2\pi\lambda_r/\lambda_i) = 0.12$ . The spaghettis starting from a non-zero  $x = x_s$  value have the same  $(t', z')$  behaviour, spiralling toward  $(t' = 0, z' = 0)$ , while they are escaping exponentially in  $x$  direction, with a factor  $\exp(4\pi\lambda_r/\lambda_i) = (1/0.12)^2$  for each loop.

Despite this topological curiosity, the electromagnetic field around the zero-field point has a linear behaviour, as expected. Indeed, the absolute *characteristic parameter*  $\eta$  we have introduced has a constant value of  $2\pi/\lambda_i$  for each loop. As the temporal and spatial sizes of the loop are proportional to the distance to the center of the whirl, the field amplitudes (Eq. (6) of the letter) are proportional to this distance.

In order to control these computations, the field components can be computed back from absolute ES lines

with  $\eta$  parameter, using Eqs. (6) of the letter, and Eqs. (25, 26), we calculate

$$\begin{pmatrix} H_y \\ D_x \end{pmatrix} = \frac{d}{d\eta} \begin{pmatrix} t' \\ z' \end{pmatrix} \quad (28)$$

$$D_z = -\frac{dx'}{d\eta} \quad (29)$$

The component  $D_z$  is the simplest to calculate : We obtain  $\lambda_x x_s e^{-\lambda_x \eta} = \lambda_x x'$  which is the expected value, given by Eq. (8). The two other components are

$$\begin{pmatrix} H_y \\ D_x \end{pmatrix} = z_s e^{\lambda_r \eta} \begin{pmatrix} -\lambda_i \beta & -\lambda_r \beta \\ \lambda_r + \lambda_i \alpha & \lambda_r \alpha - \lambda_i \end{pmatrix} \begin{pmatrix} \cos \lambda_i \eta \\ \sin \lambda_i \eta \end{pmatrix} \quad (30)$$

or

$$\begin{pmatrix} H_y \\ D_x \end{pmatrix} = z_s e^{\lambda_r \eta} \lambda_i \beta \begin{pmatrix} -1 & \alpha - \beta \\ 1 & \alpha - \beta \end{pmatrix} \begin{pmatrix} \cos \lambda_i \eta \\ \sin \lambda_i \eta \end{pmatrix} \quad (31)$$

Inverting Eq. (25) we obtain

$$z_s e^{\lambda_r \eta} \begin{pmatrix} \cos \lambda_i \eta \\ \sin \lambda_i \eta \end{pmatrix} = \frac{1}{\beta} \begin{pmatrix} \alpha & \beta \\ -1 & 0 \end{pmatrix} \begin{pmatrix} t' \\ z' \end{pmatrix}, \quad (32)$$

and eventually

$$\begin{pmatrix} H_y \\ D_x \end{pmatrix} = \lambda_i \begin{pmatrix} -2\alpha + \beta & -\beta \\ \beta & \beta \end{pmatrix} \begin{pmatrix} t' \\ z' \end{pmatrix}, \quad (33)$$

which is indeed the expected field component, given by Eq. (7).

## II. MAGNETIC FLUX ON A TUBE WALL OF ES BUNDLE IN A VACUUM IS ZERO



FIG. 2. A schematic presentation of an infinitesimal piece of the magnetic flux tube based on an ES bundle (ESs in green). The magnetic flux on  $\tau_S \wedge \kappa$  is zero, where  $\kappa$  can be any arbitrary vector not parallel to  $\tau_S$ .

The surface tangent to an ES, defined by the vector  $\tau_S = H_y \partial_t - D_z \partial_x + D_x \partial_z$ , is  $\Delta = \tau_S \wedge \kappa$ , where  $\kappa = \alpha \partial_t + \beta \partial_x + \gamma \partial_z$  is an arbitrary vector (not parallel to  $\tau_S$ ) of 2+1D spacetime.

$$\Delta = (-\beta H_y - \alpha D_z) \partial_x \wedge \partial_t + (\alpha D_x - \gamma H_y) \partial_z \wedge \partial_t + (\beta D_x + \gamma D_z) \partial_z \wedge \partial_x. \quad (34)$$

Applying the Faraday form  $F = E_x dx \wedge dt + E_z dz \wedge dt + B_y dz \wedge dx$  to bivector  $\Delta$  we obtain the magnetic flux on it

$$F(\Delta) = E_x(-\beta H_y - \alpha D_z) + E_z(\alpha D_x - \gamma H_y) + B_y(\beta D_x + \gamma D_z), \quad (35)$$

which is clearly zero in a vacuum ( $\varepsilon_0 \mu_0 = 1$ ). In conclusion, the walls of a tube made of ES bundle (Fig. 2) contain zero magnetic flux.

### III. LORENTZ INVARIANCE OF THE ESS

There is three electromagnetic approaches of the electromagnetic field, with different levels of abstraction: the vector approach with  $\mathbf{E}, \mathbf{B}, \mathbf{H}, \mathbf{D}$  vectors, the tensor-components approach, with the Faraday  $F^{ij}$  and Maxwell  $\mathcal{G}^{ij}$  tensors, and the 2-form approach, where  $F = -\frac{1}{2}F_{ij}dx^i \wedge dx^j$  and  $\mathcal{G} = \frac{1}{2}\mathcal{G}_{ij}dx^i \wedge dx^j$ . This last approach, used in the paper, constructs in an direct way the absolute topology of the ESSs, independent of any frame of reference. In the context of flat spacetime (no gravity), it is equivalent to say that the ESSs are invariant under Lorentz transformation. Here we prove this invariance with tensor components approach and with explicit computation of the  $\mathbf{H}, \mathbf{D}$  components transformation.

The vector  $\tau = \begin{pmatrix} H_y \\ -D_z \\ 0 \\ D_x \end{pmatrix}$  (Eq. (3) in the main

text) that construct a piece of spaghetti  $\begin{pmatrix} \delta t \\ \delta x \\ \delta y \\ \delta z \end{pmatrix} = \tau \delta \eta$

(Eq. (4) in the main text) is the opposite of the third column of the tensor

$$\mathcal{G}^{ij} = \begin{pmatrix} 0 & -H_x & -H_y & -H_z \\ H_x & 0 & D_z & -D_y \\ H_y & -D_z & 0 & D_x \\ H_z & D_y & -D_x & 0 \end{pmatrix}, \quad (36)$$

i.e.  $\tau = -\mathcal{G}^{iy}$ . Defined from a tensor, it is a vector, that define the piece of spaghetti independently of any frame of reference.

To give of concrete demonstration, the spaghetti segment is

$$\begin{pmatrix} \delta t \\ \delta x \\ \delta y \\ \delta z \end{pmatrix} = \begin{pmatrix} H_y \\ -D_z \\ 0 \\ D_x \end{pmatrix} \delta \eta \quad (37)$$

in a given frame of reference.

Considering another frame of reference, moving in the  $xz$  plane with the arbitrary speed components  $\beta_x$  and  $\beta_z$ ,

the Lorentz transformation matrix is

$$\Lambda = \begin{pmatrix} \gamma & -\gamma\beta_x & 0 & -\gamma\beta_z \\ -\gamma\beta_x & 1 + (\gamma - 1)\frac{\beta_x^2}{\beta^2} & 0 & (\gamma - 1)\frac{\beta_x\beta_z}{\beta^2} \\ 0 & 0 & 1 & 0 \\ -\gamma\beta_z & (\gamma - 1)\frac{\beta_x\beta_z}{\beta^2} & 0 & 1 + (\gamma - 1)\frac{\beta_z^2}{\beta^2} \end{pmatrix}, \quad (38)$$

with  $\gamma = 1/\sqrt{1 - \beta^2}$  the Lorentz factor.

In this new frame of reference, the spaghetti segment

vector coordinates are  $\begin{pmatrix} \delta t' \\ \delta x' \\ \delta y' \\ \delta z' \end{pmatrix} = \Lambda \begin{pmatrix} \delta t \\ \delta x \\ \delta y \\ \delta z \end{pmatrix}$ . As the field

components transformations use the same  $\Lambda$  matrix for

the vector  $\tau$ :  $\begin{pmatrix} H'_y \\ -D'_z \\ 0 \\ D'_x \end{pmatrix} = \Lambda \begin{pmatrix} H_y \\ -D_z \\ 0 \\ D_x \end{pmatrix}$ , we have - as ex-

pected -  $\begin{pmatrix} \delta t' \\ \delta x' \\ \delta y' \\ \delta z' \end{pmatrix} = \begin{pmatrix} H'_y \\ -D'_z \\ 0 \\ D'_x \end{pmatrix} \delta \eta$ . The spaghetti construc-

tion, with the characteristic parameter  $\eta$  is then invariant under Lorentz transformation in the  $xz$  plane.

### IV. DIRECT AND INDIRECT ESS AND ZEFSS CONSTRUCTION

As it is pointed out in the letter, in a region of no electric charge the electric flux value between two ZEFSSs is the same along any spaghetti segment. If a  $(O, \mathbf{t}, \mathbf{x}, \mathbf{z})$  frame of reference is chosen, using the zero electric flux value property of a ZEFSS, the components of the electromagnetic fields between two ZEFSS can be found as the ratio of  $d\varphi_e$  over the distances  $dt$ ,  $dx$  and  $dz$  in the directions  $\mathbf{t}, \mathbf{x}, \mathbf{z}$  with the appropriate signs

$$H_y = \frac{\partial \varphi_e}{\partial t}, \quad D_z = \frac{\partial \varphi_e}{\partial x}, \quad D_x = -\frac{\partial \varphi_e}{\partial z}. \quad (39)$$

Considering the  $\varphi_e$  potential and Eq. (39) with the curl equation  $\partial_t B_y - \partial_x E_z + \partial_z E_x = 0$  considerably simplifies a  $y$ -invariant  $p$ -polarized electromagnetic problems with no charge. In a vacuum, the resulting equation is just the d'Alembertian equal to zero:  $(\partial_t^2 - \partial_x^2 - \partial_z^2)\varphi_e = 0$  with the normal derivative Using this equation, ZEFSSs can be built directly.

The indirect method starts by the computation of the magnetic and electric field components. Two numerical techniques were used, One, with Wolfram Mathematica notebook in repository <https://github.com/marinyakovleva/spaghetti>, describe the field using the truncated Rayleigh expansion above and below the slits, the truncated exact modal expansion in the slit region. A second, with Julia notebook in repository <https://github.com/fp4code/arxiv-2208.11461>, describe the field on regular mesh in  $x$  direction and modal expansion in  $z$  direction.

The ESs lines are computed using Eq. (4) in the paper, the 2D plots of ZEFs in the middle slit plane at  $x = x_0$

where computed using a similar equation, but with vector

$$\tau_Z = D_x \partial_t + H_y \partial_z, \quad (40)$$

The electric flux used to determine different starting points of ZEFs was computed using Eq. (5), and the starting points of ESs were a selection of events where ESs and ZEFs tangent vectors are (parallel) light-like.